Journal of
Mechanics of
Materials and Structures

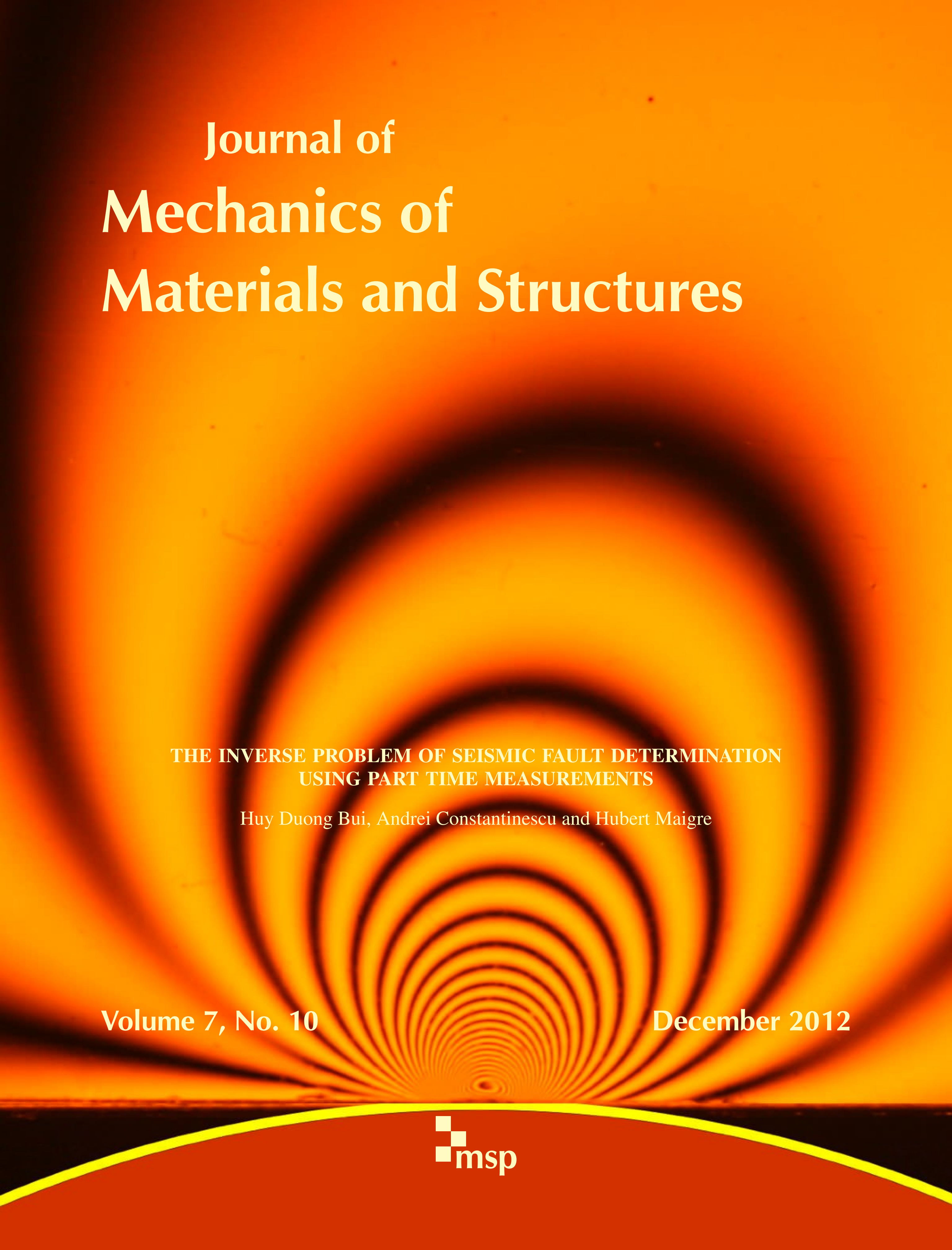

THE INVERSE PROBLEM OF SEISMIC FAULT DETERMINATION USING PART TIME MEASUREMENTS

Huy Duong Bui, Andrei Constantinescu and Hubert Maigre

Volume 7, No. 10 December 2012

msp

JOURNAL OF MECHANICS OF MATERIALS AND STRUCTURES
Vol. 7, No. 10, 2012
dx.doi.org/10.2140/jomms.2012.7.997

THE INVERSE PROBLEM OF SEISMIC FAULT DETERMINATION USING PART TIME MEASUREMENTS

HUY DUONG BUI, ANDREI CONSTANTINESCU AND HUBERT MAIGRE

This paper shows how a part time measurement T of the acceleration on the ground can be done to avoid the consideration of reflections of seismic waves on the Moho discontinuity. A bounded hemispherical solid is considered with radius greater than $c_p T$, but smaller than the Moho depth, in order to get the null boundary conditions on the hemispherical surface. The inverse problem to determine the fault plane and the time-dependent fault geometry is well-defined and solved in closed form by the reciprocity gap functional method. Two formulae are established for the components of the fault slip, which involve time and spatial Fourier transforms of some quantities related to the reciprocity gap functional. A forward initial boundary value problem in elastodynamics enables us to get the internal wave field, the shear stress as well as the normal stress on the fault. This full solution would be useful for understanding the friction mechanism on the fault during a real strike, whenever the initial uniform tectonic stresses are known from geophysical considerations.

1. Introduction

The determination of the characteristics of an earthquake from measurements of the acceleration[1]

$$\partial_t \partial_t (\boldsymbol{u})(\boldsymbol{x}, t)$$

on the stress-free ground G is one important seismic inverse problem in geophysics [Aki and Richards 1980]. Mathematically, one has to determine the fault history $\Sigma(t)$, its plane and geometry, the slip and the shear stress released from ground measurements, without considering the physical friction mechanisms at the origin of the strike. Physical models of earthquakes are not considered in this paper (for a review of such models, see [Madariaga et al. 2000]). We need a model which is generally an elastic one, bounded or unbounded and some assumption on the seismic process. Due to tectonic stresses, it is generally assumed that the release of the shear stress, completely or incompletely, corresponds to some unknown amount of tangential slip $[[\boldsymbol{u}]]$. In some cases, the fault plane is already known, for example when the slip occurs in existing plane (San Andreas fault) or when the slip plane emerges on the ground. The analysis of data in view of the inversion is simpler in these cases.

Before introducing the aim of the paper, we briefly review some methods of earthquake inverse problems in order to see what can be improved.

In simple cases listed above, some *forward* models in infinite elastic medium can give good prediction of the acceleration signals to be compared to measurements [Campillo 1983; Cochard and Rice 1997; Vallée 2003; Peyrat et al. 2004; Lapusta et al. 2001]. True *inverse* problems are divided into two kinds.

Keywords: earthquake, inverse problem, reciprocity gap, elastic wave, fault history.

[1] We use the notation $\partial_t = \partial/\partial t$.

In the first one, a feedback between forward models of faults and observations is made to determine the optimal solution [Das and Kostrov 1990; Das and Suhadolc 1996]. Most papers on inverse problems in seismology are based on this optimization method (or geometry control method). The method has some advantage, since it is based on numerical approaches for which powerful finite element software exist. However, there are also some limitations because of the ill-posedness of inverse problems, for which analytical solutions are missing. According to Das and Suhadolc [1996], the least-squares functional (for fitting the computed acceleration from a guess fault S with the measured one $\boldsymbol{a}$)

$$J(S(\tau)) = \|\partial_\tau \partial_\tau \boldsymbol{u} - \boldsymbol{a}\|_u^2 + \alpha \|\partial_\tau \boldsymbol{u}\|_{\partial S}^2, \tag{1}$$

$$\Sigma(t) = \arg \min_{S(\tau)} J(S(\tau)), \tag{2}$$

with possible additional regularizing term with $\alpha > 0$ to bound the velocity of the fault front ∂S, has a flat minimum in the $\boldsymbol{u}$ space.

The same authors give a clear statement on such an optimal solution: "*Even if the fitting of data seems to be quite good, the faulting process is poorly reproduced, so that in the real case, it would be difficult to know when one has obtained a correct solution.*"

In the second kind of method, introduced by the authors and their colleagues for many kinds of inverse problems in solid and fracture mechanics, ranging from elastostatics [Andrieux et al. 1999] to heat diffusion in solids, acoustics and elastodynamics, with the earthquake-like analysis (see the reviews in [Bui 2006]), the original *nonlinear* inverse problems with respect to the unknowns considered *together*, is put in a special variational form which enables us to determine the unknowns *separately* in a certain order: first the normal to the fault plane $\boldsymbol{N}$, then the fault plane and finally the fault geometry. Each subproblem is characterized by the use of a specific adjoint field. More importantly, the subvariational equations are *linear* or quasilinear (this word will be explained in Section 3) with respect to the considered unknowns. Therefore, the original nonlinear inverse problem is decomposed into *successive linear* inverse problems which are solved analytically in a certain order.

In previous works, models have been worked out for some earthquake inverse problems, which differ by physical considerations and methods of solution. First, to avoid reflection of waves in the underground discontinuities, by considering the near field only and assuming certain shape of the source, one can obtain signals to be compared to observations [Campillo 1983]. An earthquake *like* model assumes that the bounded solid is entirely elastic and that data are available in its whole boundary. Such a model does not apply to real earthquake, because data cannot be obtained in the underground, but has the advantage of giving an exact solution to the fault history $\Sigma(t)$ [Bui et al. 2005]. The second approximate model which also determines the full history of the fault considers a semi infinite elastic medium, for which it is necessary to specify the far-field radiated by the earthquake [Vallée 2003], which can be estimated approximately. Both models give the entire fault history described by the displacement jump across the fault $[[\boldsymbol{u}]] = \boldsymbol{u}^+ - \boldsymbol{u}^-$, a function of $(\boldsymbol{x}, t)$ and suppose an infinite duration of the acceleration measurement $\boldsymbol{a}$. The method is based on the use of adjoint fields $\boldsymbol{v}(\boldsymbol{x}, t)$ to establish a variational equation for the current discontinuous elastodynamic field $\boldsymbol{u}(\boldsymbol{x}, t)$ called *reciprocity gap functional* (Section 2).

Regarding the actual seismic process, the physical models above are not realistic. In a real process, waves travel in the crust, then reflect on and diffract through the Mohorovičić discontinuity; see Figure 1. Suppose that the crust has a depth of 60 km, P-waves from a point source near the ground will take

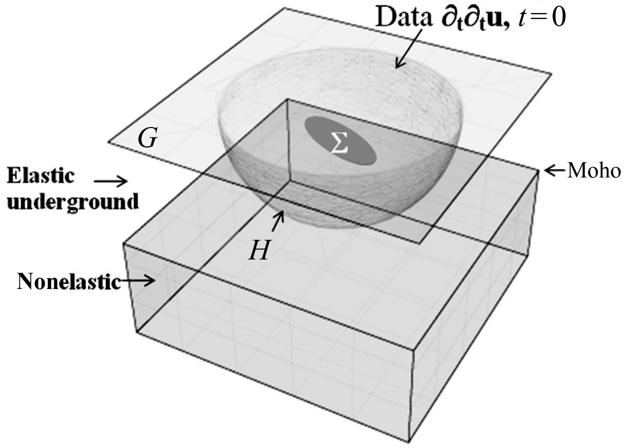

Figure 1. The seismic model. Part time measurement of the acceleration on the stress-free ground G, inside a circular area of radius $c_p T$ during the time T; H is a hemispherical surface tangent to the Mohorovičić discontinuity containing a small fault Σ near the ground. All seismic signals are inside the elastic hemisphere, for $0 < t < T$.

about 10 s to reach the Moho discontinuity. Beyond this time, after 20 s, reflected waves arrive on the ground so that measured data correspond to so many sources, the fault and the Moho interface. So the question is: what part of the signal can be used for the reconstruction of the wave due to the strike only? A two-dimensional simulation of a sudden release of shear stress over a small fault located near the free surface is shown in Figure 2. It is observed that complex waves, P-waves, S-waves and intermediate waves are generated, as predicted [Hudson 1980]. Numerical solutions are much more complex when the reflection of waves occurs at the interface. Ghost solutions are observed near the ground which explain the difficulty encountered in numerical optimization methods [Das and Suhadolc 1996].

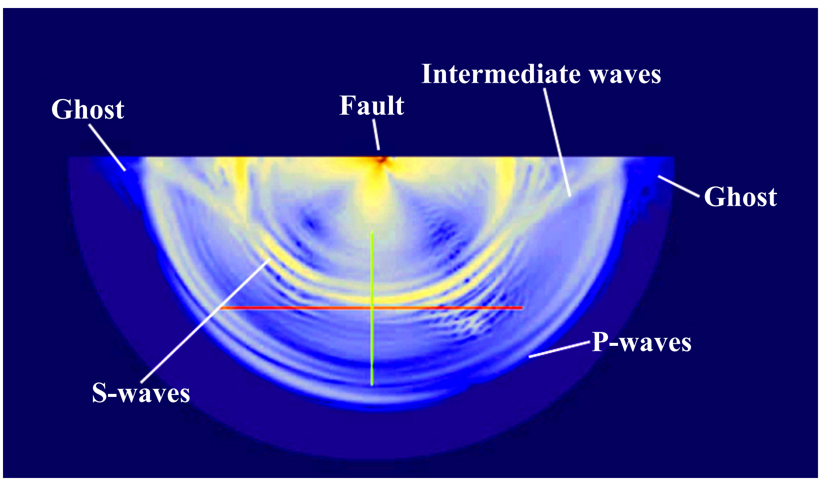

Figure 2. A two-dimensional numerical simulation of an earthquake by the sudden release of shear stress on a small fault near the ground, showing ghost solution.

Now, consider a finite duration T such that P-waves from the source do not reach the Moho discontinuity, the depth of which is more or less known from geophysical considerations. Take any volume or a hemisphere with boundary H in the elastic region above the Moho discontinuity, with radius larger than $c_p T$ but smaller than the Moho discontinuity depth, containing the perturbation field. We then know the boundary fields on H:

$$\boldsymbol{u} = \boldsymbol{0} \quad \text{and} \quad \boldsymbol{T} = \boldsymbol{\sigma}[\boldsymbol{u}].\boldsymbol{n} = \boldsymbol{0} \quad \text{on } H \times [0, T]. \tag{3}$$

The aim of the paper is to show how to solve analytically the nonlinear inverse problem, using *partial* information on the ground acceleration, conditions of (3) and the *a priori* knowledge on the planar character of slip fault. No uncertainties of data are considered in this paper. The smaller the time T, the shorter the history of the strike which can be recovered. We shall assume first that acceleration data are due to some rapid release of shear stresses on the moving fault faces. The assumption is based on the experimental evidence of shear cracks faster than the shear wave speed which has been reported in [Rosakis et al. 1999], $c_s < V \leq \sqrt{2} c_s$. Actually, the only assumed boundary condition on the fault is that it is a planar shear fault. We do not know how the shear stresses are released, or what the fault speed is. We shall show that a rigorous mathematical analysis will solve the inverse problem in closed form, giving the fault plane in Section 3. Section 4 discusses a proposal to determine the fault history $\Sigma(t)$ and establishes two formulae giving the components of the displacement jump explicitly. The solution allows the determination of the release stress on the fault via a forward initial and boundary value problem in elastodynamics. A complete solution of the inverse problem, giving both the shear stress and the slip components on the fault, would be helpful for understanding the friction law mechanism. This paper examines the mathematical aspects of such an inverse problem.

2. The reciprocity gap functional

Since waves travel in the crust of finite depth we shall consider a *finite* duration T for the analysis of the inverse problem. The physical model is based on the following assumptions. At initial time, a sudden shear slip or a release of (unknown) shear stress over the fault faces $\Sigma^{\pm}$ generates elastic waves which can be measured on the stress-free ground. No stresses are applied to the external boundary of the solid. Such conditions have been considered in our earthquake-like model [Bui et al. 2005]. No reflections of waves occur yet at the Moho discontinuty during the time T and (3) holds. No other assumptions will be needed except that measurements of the acceleration (a time-dependent vector field) on the ground are done on the perturbed area up to T.

For the self-consistency of the paper, we reestablish the general expression of the reciprocity gap functional R and its particular expression for the present study for a finite duration time of measurements. Let Ω be the elastic region before the quake, with boundary $\partial\Omega = G \cup H$. After the quake, the sound region is $\Omega' = \Omega \setminus \Sigma$, with boundary $\partial\Omega' = G \cup H \cup \Sigma^{\pm}$. We shall denote the region occupied by the current wave by Ω''. Its boundary is the convex hull generated by spherical P-waves of radius $c_p T$ emitted by all points of the fault.

The current elastodynamic displacement field $\boldsymbol{u}(\boldsymbol{x}, t)$ due to either the release of shear stress on $\Sigma^{\pm}$ or the imposition of the tangential jump $[[\boldsymbol{u}]]$ on a plane of normal $\boldsymbol{N}$ satisfies the equation of motion, initial conditions and boundary conditions (L is the isotropic elastic moduli tensor, ρ is the density) as follows:

$$\operatorname{div}(L:\operatorname{grad}(\boldsymbol{u}))-\rho\partial_t\partial_t\boldsymbol{u}=\boldsymbol{0}\quad\text{on } (\Omega\setminus\Sigma)\times[0,T], \tag{4}$$

$$\boldsymbol{u}(\boldsymbol{x},0)=\boldsymbol{0},\quad \partial_t\boldsymbol{u}(\boldsymbol{x},0)=\boldsymbol{0}\quad\text{in } (\Omega\setminus\Sigma), \tag{5}$$

$$\partial_t\partial_t\boldsymbol{u}=\boldsymbol{a}\quad\text{on } G\times[0,T], \tag{6}$$

$$\boldsymbol{T}=\sigma[\boldsymbol{u}].\boldsymbol{n}=\boldsymbol{0}\quad\text{on } G\times[0,T], \tag{7}$$

$$\boldsymbol{T}=\sigma[\boldsymbol{u}].\boldsymbol{n}=\boldsymbol{0}\quad\text{on } H\times[0,T], \tag{8}$$

$$\boldsymbol{u}=\boldsymbol{0}\quad\text{on } H\times[0,T], \tag{9}$$

$$[\![\boldsymbol{u}]\!].\boldsymbol{n}=\boldsymbol{0}\quad\text{on } \Sigma^{\pm}. \tag{10}$$

The adjoint field $\boldsymbol{v}$ is continuous throughout Ω and satisfies the wave equation and the final conditions

$$\operatorname{div}(L:\operatorname{grad}(\boldsymbol{v}))-\rho\partial_t\partial_t\boldsymbol{v}=\boldsymbol{0}\quad\text{in } \Omega\times[0,T], \tag{11}$$

$$\boldsymbol{v}(\boldsymbol{x},t=T)=\boldsymbol{0},\quad \partial_t\boldsymbol{v}(\boldsymbol{x},t=T)=\boldsymbol{0}\quad\text{in } \Omega. \tag{12}$$

Multiply (4) by $\boldsymbol{v}$, (11) by $\boldsymbol{u}$, subtract the result, then integrate the final result in $\Omega'\times[0,T]$ where $\boldsymbol{N}$ is the normal to the fault ($\boldsymbol{N}$ is also the normal to Σ^-)

$$\int_0^T\int_\Sigma [\![\boldsymbol{u}]\!].\sigma[\boldsymbol{v}].\boldsymbol{N}\,dt\,dS+\int_0^T\int_{\Omega'}\rho\frac{\partial}{\partial t}(\boldsymbol{u}\partial_t\boldsymbol{v}-\boldsymbol{v}\partial_t\boldsymbol{u})\,dt\,dV=R(\text{data},\boldsymbol{v}), \tag{13}$$

where

$$R(\text{data},\boldsymbol{v})\stackrel{\text{def}}{=}\int_0^T\int_G \boldsymbol{u}.\sigma[\boldsymbol{v}].\boldsymbol{n}\,dt\,dS. \tag{14}$$

We have

$$\int_0^T\int_{\Omega'}\rho\frac{\partial}{\partial t}(\boldsymbol{u}.\partial_t\boldsymbol{v}-\boldsymbol{v}.\partial_t\boldsymbol{u})\,dt\,dV=\int_{\Omega'}dV\rho(\boldsymbol{u}.\partial_t\boldsymbol{v}-\boldsymbol{v}.\partial_t\boldsymbol{u})\,|_0^T\,. \tag{15}$$

Using the initial conditions on $\boldsymbol{u}$ and the final conditions on $\boldsymbol{v}$ we obtain

$$\int_{\Omega'}dV\rho(\boldsymbol{u}.\partial_t\boldsymbol{v}-\boldsymbol{v}.\partial_t\boldsymbol{u})\,|_0^T=0. \tag{16}$$

Finally the variational equation for the inverse problem is given by

$$\int_0^T\int_\Sigma [\![\boldsymbol{u}]\!].\sigma[\boldsymbol{v}].\boldsymbol{N}\,dt\,dS=R(\text{data},\boldsymbol{v})\quad\text{for all }\ \boldsymbol{v}. \tag{17}$$

$R(\text{data},\boldsymbol{v})$ is called the *reciprocity gap functional*, which measures the *symmetry loss* between $\boldsymbol{u}$ and $\boldsymbol{v}$. It depends on the acceleration data $\boldsymbol{a}$ on the ground. By a time integration of $\boldsymbol{a}$, twice, we get the surface field $\boldsymbol{u}(\boldsymbol{x},t)$ over G for the right side of (14).

As a matter of fact, the origin of time has been taken at the origin of the hidden source strike. Recorded acceleration signals start when the first strike arrives at the ground with some delay t_1. The true origin of time takes account of this delay, equal to $t_1=(c_p/c_s-1)\Delta$ with the difference Δ between the arrival times of the first S-wave and P-wave.

3. Adjoint fields to determine the fault plane

The adjoint fields $\boldsymbol{v}(\boldsymbol{x}, t)$ to be considered will depend on parameters (scalar, vector, tensor). They are either plane S-shear waves or plane P-waves, with the moving front Γ propagating in the $\boldsymbol{p}$ direction, with respective velocity $c = c_s$ or $c = c_p$. There is a smooth transition of $\boldsymbol{v}(\boldsymbol{x}, t)$ from the zero value behind the wave to the one in front of the wave, in a narrow band of width $w > 0$, $w \to 0$. Adjoint P-waves are discussed later. Adjoint S-waves polarized in the direction $\boldsymbol{k}$ are proportional to the regularized (smooth) Heaviside function $Y^w(\boldsymbol{x}.\boldsymbol{p}/c - t - \tau)$, where τ is a parameter fixing the initial position of the wave front, denoted by Γ^τ, w is a positive number tending to zero ($Y(y) = 1$ for $y > w$ and $Y(y) = 0$ for $y < 0$)

$$\boldsymbol{v}(\boldsymbol{x}, t; \tau, \boldsymbol{p}) = Y^{+0}(\boldsymbol{x}.\boldsymbol{p}/c_s - t - \tau)\boldsymbol{k}. \tag{18}$$

They satisfy the homogeneous wave equation in $(\Omega \setminus \Gamma) \times [0, T]$ and depend on the scalar τ and vectors $\boldsymbol{p}$ and do not have discontinuities across the fault. The adjoint stress in the band tends to an impulse as the width $w > 0$ tends to zero. R becomes the *instantaneous reciprocity gap* introduced in [Bui et al. 2004].

The fault plane. The choice of the propagating direction $\boldsymbol{p}$ for adjoint S-waves must satisfy (16). Figures 3 and 4(b) show that adjoint S-waves can be considered near the top A of the fault only, with fronts more or less inclined with the angle α with respect to the horizontal plane, with the maximum angle $\alpha_{\max}$ which depends on the depth d of point A. The existence of a maximum angle is explained by the fact that an S-wave is slower than a P-wave and that possibly the final condition (12) cannot be satisfied for large angle. If the front has a steep angle, the S-wave at time T has a nonempty intersection with the domain Ω'', so (16) is not satisfied:

$$0 \le \alpha < \alpha_{\max} = a\sin\frac{c_s}{c_p} - a\sin\frac{d}{T c_p}. \tag{19}$$

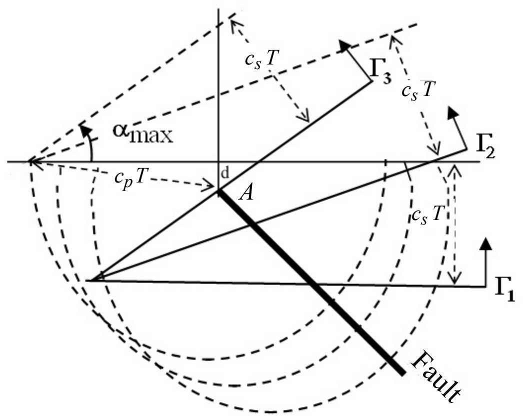

Figure 3. Adjoint S-waves propagating upwards. The angles between the propagating vectors and the vertical depend on the depth d of the nearest point A to the ground. The maximun angle is for the front Γ_3, the minimum (zero value) for the front Γ_1.

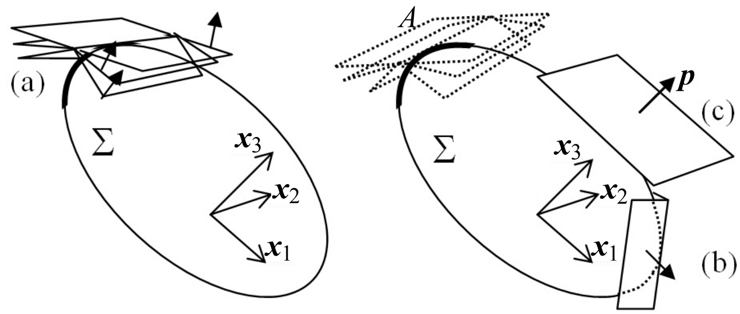

Figure 4. Left: adjoint S-waves propagating upwards (a) with different $\boldsymbol{p}$ under some angle constraints for determining the tangents to the fault front near point A. Right: P-waves of arbitrary propagation vectors (b) can also be used for determining the fault plane. A P-wave parallel to the fault plane (c) is used to determine the fault geometry.

Adjoint P-waves of arbitrary propagation vectors $\boldsymbol{p}$ can also be considered for determining the fault plane; see label (b) in Figure 4. Once the fault plane has been determined, a particular wave parallel to the fault can be used for determining the geometry; see label (c) in the same figure.

The apex of point A can be determined by geometrical considerations of the first waves reaching the ground. It can also be determined directly by horizontal adjoint waves of type Γ_1 by changing τ. First choose τ so that the fault is entirely behind the wave front, thus $\sigma[\boldsymbol{v}] = 0$ on the fault or the integral in the left side of (17) vanishes, hence $R = 0$. Then change τ so that $R \neq 0$. The transition of R from zero (for large τ) to a non zero value indicates that the adjoint wave front is tangent to the fault boundary.

Let us consider now a wave front of the type Γ_2 of Figure 3, the initial position of which is near to point A. By changing τ we change its initial position and by changing $\boldsymbol{p}$ we change its orientation, also to get the transition from zero to a nonzero value of R revealing the contact point and the tangents to the fault front $\partial\Sigma$. Therefore by trials and errors with this *zero-crossing* method, we determine a small three-dimensional curve of the fault front near the point A. This is sufficient to get the entire fault plane.

Remark that we do not make the assumption of a global convex shape of the fault plane, but only a locally convex front; see Figure 4. The zero-crossing method is the same as the one considered for a line crack in 2 dimensions [Bui et al. 2004], which is illustrated in Figure 5 where the zero-crossing has been appreciated with a small number. Having determined the fault plane, we take the axes Ox_1x_2 on the fault plane and $\boldsymbol{N} = \boldsymbol{e}^3$.

In our previous method to determine the normal $\boldsymbol{N}$, we considered an adjoint field such that the stress $\sigma[\boldsymbol{v}]$ is constant everywhere, so that (17) can be written as

$$\boldsymbol{N}.\sigma[\boldsymbol{v}].\left(\int_0^{-\tau}\int_\Sigma [[\boldsymbol{u}]]\,dt\,dS\right) = R(\text{data}, \boldsymbol{v}) \quad \text{for all } \boldsymbol{v},$$

which is quasilinear in $\boldsymbol{N}$, because Σ still depends on $\boldsymbol{N}$. However, using an argument given in [Andrieux et al. 1999] we can show that two independent data are necessary and sufficient to determine the direction of the normal which is linked to the eigenvectors of the tensor Z^{ij} of components $R(\boldsymbol{v}^{ij})$, without knowing Σ and $[[\boldsymbol{u}]]$. Unfortunately, this analytical method is useless for the seismic inverse problem because the seismic event is unique.

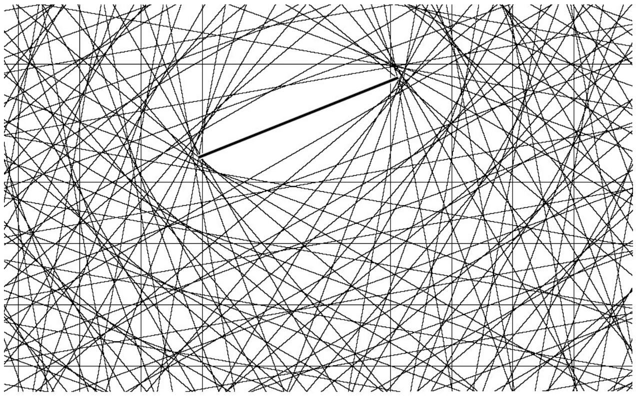

Figure 5. Instantaneous adjoint S-waves for determining the convex hull of a line crack [Bui et al. 2004].

4. The partial fault history

We need another kind of adjoint P-waves and S-waves, which allows the components $[[u_1]]$, $[[u_2]]$ to be calculated separately, but under some additional assumptions. Moreover, new adjoint waves allow the determination of the partial fault history $\Sigma(t)$ for $0 < t < T$.

The reciprocity gap functional is rewritten below

$$\int_0^T \int_\Sigma [[\boldsymbol{u}]].\sigma[\boldsymbol{v}].\boldsymbol{N}\, dt\, dS + \int_{\Omega'} dV[\rho(\boldsymbol{u}.\partial_t \boldsymbol{v} - \boldsymbol{v}.\partial_t \boldsymbol{u})]\,|_0^T = R(\text{data}, \boldsymbol{v}) \quad \text{for all } \boldsymbol{v}. \tag{20}$$

The additional assumption. In the second integral, denoted by K, the term for $t = 0$ already vanishes because of the initial conditions on $\boldsymbol{u}$. We make the assumption that second term for $t = T$ can be omitted for a particular adjoint field. More precisely, for fixed T and for any given positive number ϵ, *as small as* we want, we can find a particular adjoint field such that

$$K = \int_{\Omega'} dV[\rho(\boldsymbol{u}.\partial_t \boldsymbol{v} - \boldsymbol{v}.\partial_t \boldsymbol{u})]\,|_0^T = O(\epsilon) \tag{21}$$

instead of $K = 0$, (16). The additional assumption is based on two arguments: firstly a natural and small damping of the medium exists so that the wave equation is only an approximated one,[2] secondly adjoint fields $\boldsymbol{v}$ having a good behavior at large time (rapid decay with time) can be easily found.

We study the geometry of the moving fault $\Sigma(t)$ with the coordinates attached to the fault plane $x_3 = 0$. Consider functions F depending on parameters ($\boldsymbol{s} \in \mathbb{R}^2$, $q \in \mathbb{R}$), satisfying the scalar wave equation for $0 < t < T$ (and $F = 0$ otherwise) of the form

$$F(\boldsymbol{x}, t; \boldsymbol{s}, q, c) = \exp((iq - k)t) \exp(i\boldsymbol{s}.\boldsymbol{x}) \exp\Big(x_3\Big[\|s\|^2 + \frac{(iq-k)^2}{c^2}\Big]^{1/2}\Big), \tag{22}$$

[2]To take account of a small damping, a term such as $-\eta\partial_t \boldsymbol{u}$ ($\eta > 0$) can be added to the left side of (4) and the corresponding antidamping term $+\eta\partial_t \boldsymbol{v}$ to (11), the assumption becomes $\int_{\Omega'} dV[\rho(\boldsymbol{u}.\partial_t \boldsymbol{v} - \boldsymbol{v}.\partial_t \boldsymbol{u}) - \eta \boldsymbol{u}.\boldsymbol{v}]\,|^{t=T} = O(\epsilon)$.

with positive $k > 0$ chosen so that $\exp(-kT) = \epsilon$ and $c = c_p$ for P-waves and $c = c_s$ for S-waves.[3] Adjoint waves that are proportional to F have a good behavior at large time T as $\exp(-kT)$. The term $\exp(x_3)\|s\|^2$ is finite in the bounded medium. Two adjoint waves are considered, one for P-waves and the other for S-waves:

$$\boldsymbol{v}^{(p)} = \operatorname{grad} F(\boldsymbol{x}, t; \boldsymbol{s}, q, c_p), \quad \boldsymbol{v}^{(s)} = \operatorname{curl} F(\boldsymbol{x}, t; \boldsymbol{s}, q, c_s)\boldsymbol{e}^3. \tag{23}$$

The components of the slip. Equation (17) gives two linear systems of equations, with $x_3 = 0$ on the left sides of the equations, for $\boldsymbol{D} \overset{\text{def}}{=} [\![\boldsymbol{u}]\!]$:

$$\int_{x_3=0}\int_0^T [is_1 D_1 + is_2 D_2]\exp((iq-k)t)\exp(i\boldsymbol{s}.\boldsymbol{x})\,dt\,dS$$
$$= \frac{1}{2\mu}\Big[\|\boldsymbol{s}\|^2 + \frac{(iq-k)^2}{c_p^2}\Big]^{-1/2} R(\text{data}, \boldsymbol{v}^{(p)}(\boldsymbol{s}, q, c_p)) \overset{\text{def}}{=} iG^{(1)}(\text{data}, \boldsymbol{s}, q, c_p),$$

$$\int_{x_3=0}\int_0^T [is_2 D_1 - is_1 D_2]\exp((iq-k)t)\exp(i\boldsymbol{s}.\boldsymbol{x})\,dt\,dS$$
$$= \frac{1}{\mu}\Big[\|\boldsymbol{s}\|^2 + \frac{(iq-k)^2}{c_s^2}\Big]^{-1/2} R(\text{data}, \boldsymbol{v}^{(s)}(\boldsymbol{s}, q, c_s)) \overset{\text{def}}{=} iG^{(2)}(\text{data}, \boldsymbol{s}, q, c_s).$$

The equations defines $G^{(1)}$ and $G^{(2)}$ in terms of $R(\text{data}, \boldsymbol{v}^{(p)})$ and $R(\text{data}, \boldsymbol{v}^{(s)})$, respectively. We see that the combinations $(s_1 G^{(1)} + s_2 G^{(2)})$ and $(s_2 G^{(1)} - s_1 G^{(2)})$ are proportional to $\|\boldsymbol{s}\|^2$, so we can divide them by $\|\boldsymbol{s}\|^2$. Now define function $E(t) = \exp(-kt)$ for $0 < t < T$ and $E(t) = 0$ otherwise. It follows that the double integral can be extended to the whole space-time. We obtain

$$\int_{x_3=0}\int_{-\infty}^{+\infty} D_1(\boldsymbol{x}, t)E(t)\exp(iqt)\exp(i\boldsymbol{s}.\boldsymbol{x})\,dt\,dS = (s_1 G^{(1)} + s_2 G^{(2)})/\|\boldsymbol{s}\|^2, \tag{24}$$

$$\int_{x_3=0}\int_{-\infty}^{+\infty} D_2(\boldsymbol{x}, t)E(t)\exp(iqt)\exp(i\boldsymbol{s}.\boldsymbol{x})\,dt\,dS = (s_2 G^{(1)} - s_1 G^{(2)})/\|\boldsymbol{s}\|^2. \tag{25}$$

Since $\boldsymbol{s} \in \mathbb{R}^2$ and $q \in \mathbb{R}$, the left sides of (24) and (25) are the double time Fourier transform F_t and spatial Fourier transform F_x of $D_1(\boldsymbol{x}, t)E(t)$ and $D_2(\boldsymbol{x}, t)E(t)$ respectively. Their right sides are known functions of data and $\boldsymbol{s}, q$.

Based on our previous works, which considered adjoint waves of the same exponential type, we know that the reciprocity gap functional is the spatial Fourier transform of a *compact support* function. For a similar inverse problem, the proof (based on the Wiener–Paley theorem) can be found in [Ben Abda and Bui 2003].

Finally, by double inverse Fourier transforms in the image spaces $(\boldsymbol{s}, q)$, we obtain each component of the displacement jump and the fault history given by its support function, $\Sigma = \operatorname{supp}([\![u_1]\!]) \cup \operatorname{supp}([\![u_2]\!])$, for $\epsilon = \exp(-kT) \to 0$:

$$[\![u_1]\!](\boldsymbol{x}, t)E(t) = F_q^{-1} F_s^{-1} \frac{s_1 G^{(1)} + s_2 G^{(2)}}{\|\boldsymbol{s}\|^2}, \quad [\![u_2]\!](\boldsymbol{x}, t)E(t) = F_q^{-1} F_s^{-1} \frac{s_2 G^{(1)} - s_1 G^{(2)}}{\|\boldsymbol{s}\|^2}. \tag{26}$$

[3] In the case of damping, we take

$$F(\boldsymbol{x}, t; \boldsymbol{s}, q, c) = \exp((iq-k)t)\exp(i\boldsymbol{s}.\boldsymbol{x})\exp\Big(x_3[\|s\|^2 + \frac{(iq-k)^2}{c^2} - \eta(iq-k)]^{1/2}\Big).$$

The released stresses. Knowing the displacement jump on the fault, the acceleration on the ground, the null displacement on H, with the initial conditions, we are left with a well-posed forward problem of elastodynamics which determines the displacement field inside the volume Ω' and the release stresses on the fault.

The knowledge of both the shear stress and the slip on the fault, could be helpful for understanding the friction law mechanism. The solution of the inverse problem and the forward one give the stress field $\sigma[\boldsymbol{u}]$, in particular the normal stress σ_{33} and the shear stress on the fault σ_{3m}, along the direction $\boldsymbol{m}$ of the fault slip. These stress components are only variations of the stress in the strike. The actual stresses to be considered in the friction law are the sum of the released stress $\sigma[\boldsymbol{u}]$ and the tectonic one Σ^{tect} provided by geophysical considerations only.

Remarks. 1. For an infinite medium or infinite time measurement $c_p T = \infty$, we have $K = 0$. The solution is the same given by (26).

2. For an explicit solution $\partial_t \partial_t \boldsymbol{u}$ and exact data $\boldsymbol{a}$ in the residual J of (1), the numerical calculation of the slip via fast Fourier transforms in space and time, followed by the calculation of the theoretical acceleration on the ground via the elastodynamic solution, always involve errors. Therefore the residual J does not vanish. This behavior is also related to the remark of Das and Suhadolc about the flat minimum of the residual (quoted on page 998).

5. Conclusions

To avoid reflections of waves in the Moho discontinuity, one generally considers either near-fields or infinite medium for studying earthquake inverse problems. We have shown that these assumptions are not necessary. Firstly, we can consider a bounded solid above the Moho discontinuity. Secondly, we have shown that a part time T of measurement of the acceleration on the ground, before seismic waves reach the boundary of the solid considered, leads to a rigorous mathematical analysis of the equations and provides the solution to the inverse problem: the fault plane and its time-dependent geometry are determined. We establish the formulae giving the components of the fault slip in terms of the ground data during the time T. Having solved the inverse problem, a forward initial and boundary value problem in elastodynamics can provide the field solution and consequently the shear stress released on the fault.

The explicit solution of the earthquake inverse problem, obtained by the reciprocity gap method, provides both the slip field and the shear stress (and also the normal stress) on the fault and would be useful to understand the seismic mechanisms, particularly to find the friction law on the active fault.

Numerical applications of the proposed method are beyond the scope of this paper and will appear in a forthcoming paper.

References

[Aki and Richards 1980] K. Aki and P. Richards, *Qauntitative seismology, theory and methods*, W.H. Freeman and Cie, New York, 1980.

[Andrieux et al. 1999] S. Andrieux, A. Ben Abda, and H. D. Bui, “Reciprocity principle and crack identification”, *Inverse Problems* **15**:1 (1999), 59–65.

[Ben Abda and Bui 2003] A. Ben Abda and H. D. Bui, “Planar crack identification for the transient heat equation”, *J. Inverse Ill-Posed Probl.* **11**:1 (2003), 27–31.

[Bui 2006] H. D. Bui, *Fracture mechanics: inverse problems and solutions*, Solid Mechanics and Its Applications **139**, Springer, 2006.

[Bui et al. 2004] H. D. Bui, A. Constantinescu, and H. Maigre, "Numerical identification of linear cracks in 2D elastodynamics using the instantaneous reciprocity gap", *Inverse Problems* **20**:4 (2004), 993–1001.

[Bui et al. 2005] H. D. Bui, A. Constantinescu, and H. Maigre, "An exact inversion formula from determining a planar fault from boundary measurements", *J. Inverse Ill-Posed Probl.* **13**:3-6 (2005), 553–565.

[Campillo 1983] M. Campillo, "Numerical evaluation of the near-field high-frequency radiation from quasi-dynamic circular fault", *Bulletin Seismological Society of America* **73** (1983), 723–734.

[Cochard and Rice 1997] A. Cochard and J. R. Rice, "A spectral method for numerical elastodynamic fracture analysis without spatial replication of the rupture event", *J. Mech. Phys. Solids* **45**:8 (1997), 1395–1418.

[Das and Kostrov 1990] S. P. Das and B. V. Kostrov, "Inversion for seismic slip rate and distribution with stabilizing constraints. Applications to the 1986 Andreanov Islands earthquake", *J. Geophys. Res.* **95** (1990), 6899–6913.

[Das and Suhadolc 1996] S. Das and P. Suhadolc, "On the inverse problem for earthquake rupture. The Haskell-type source model", *Journal of Geophysical Research* **101**:B3 (1996), 5725–5738.

[Hudson 1980] J. A. Hudson, *The excitation and propagation of elastic waves*, Cambridge Monographs on Mechanics and Applied Mathematics, Cambridge University Press, 1980.

[Lapusta et al. 2001] N. Lapusta, J. Rice, Y. Ben-Zion, and G. Zheng, "Elastodynamic analysis for slow tectonic loading with spontaneous rupture episodes on faults with rate- and state-dependent friction", *Geophys. Res.* **105** (2001), 23765–23789.

[Madariaga et al. 2000] R. Madariaga, S. Peyrat, and K. B. Olsen, "Rupture dynamics in 3D. A review", pp. 89–110 in *Problems in Geophysics for the New Millennium*, edited by E. Boschi et al., Editrice Compositori, Italy, 2000.

[Peyrat et al. 2004] S. Peyrat, K. Olsen, and R. Madariaga, "Which dynamic rupture parameters can be estimated from strong ground motion and geodesic data?", *Pure and Applied Geophysics* **161** (2004), 2155–2169.

[Rosakis et al. 1999] A. J. Rosakis, O. Samudrala, and D. Coker, "Cracks facter than the shear wave speed", *Sciences* **284**:5418 (1999), 1337–1340.

[Vallée 2003] M. Vallée, *Kinematic analysis of the earthquake with far-fields. Methods and solution*, Ph.D. thesis, Université de Grenoble, 2003.

Received 18 Oct 2012. Accepted 16 Nov 2012.

HUY DUONG BUI: hdbui37@yahoo.fr
Laboratoire de Mécanique des Solides, CNRS UMR 7649, École Polytechnique ParisTech, Route de Saclay, 91128 Palaiseau, France

and

LaMSID/UMR EDF-CNRS-CEA 2832, EDF, Clamart, France, UME Mecanique, ENSTA ParisTech, France

ANDREI CONSTANTINESCU: andrei.constantinescu@lms.polytechnique.fr
Laboratoire de Mécanique des Solides, CNRS UMR 7649, École Polytechnique ParisTech, Route de Saclay, 91128 Palaiseau, France

HUBERT MAIGRE: hubert.maigre@insa-lyon.fr
INSA-Lyon, Villeurbanne, 69621 Lyon, France

JOURNAL OF MECHANICS OF MATERIALS AND STRUCTURES

msp.org/jomms

Founded by Charles R. Steele and Marie-Louise Steele

See msp.org/jomms for submission guidelines.

JoMMS (ISSN 1559-3959) at Mathematical Sciences Publishers, 798 Evans Hall #6840, c/o University of California, Berkeley, CA 94720-3840, is published in 10 issues a year. The subscription price for 2012 is US $555/year for the electronic version, and $735/year (+$60, if shipping outside the US) for print and electronic. Subscriptions, requests for back issues, and changes of address should be sent to MSP.

JoMMS peer-review and production is managed by EditFlow® from Mathematical Sciences Publishers.

PUBLISHED BY

mathematical sciences publishers

nonprofit scientific publishing

http://msp.org/

Journal of Mechanics of Materials and Structures

Volume 7, No. 10 December 2012

1559-3959(2012)7:10;1-#